11ème Colloque sur la Physique des Collisions Atomiques et Electroniques
Metz (France), June 1986
Vol. II, invited talks
(46)

Experiments on Resonances in Electron-Molecule Scattering at Low Energies

Michael Allan

Institut de Chimie Physique de l'Université de Fribourg Suisse
1700 Fribourg, Switzerland

1. INTRODUCTION

This contribution first briefly describes a novel instrument for electron scattering studies, the trochoidal electron spectrometer. The properties of this instrument are demonstrated by showing several previously investigated spectra in nitrogen, permitting a comparison with the results obtained by the more frequently utilized electrostatic instrument.

Two investigations conducted with this instrument are then presented. One is the energy-dependence of vibrational excitation in small molecules H_2 and N_2. The second application of the new instrument is the observation of the resonant autodetachment channel in the decay of Feshbach resonances in organic molecules.

2. TROCHOIDAL ELECTRON SPECTROMETER

The instrument has been described previously [1], and is shown schematically in Figure 1. It uses trochoidal analysers both to prepare a beam of monoenergetic electrons and to analyse the energies of the scattered electrons.

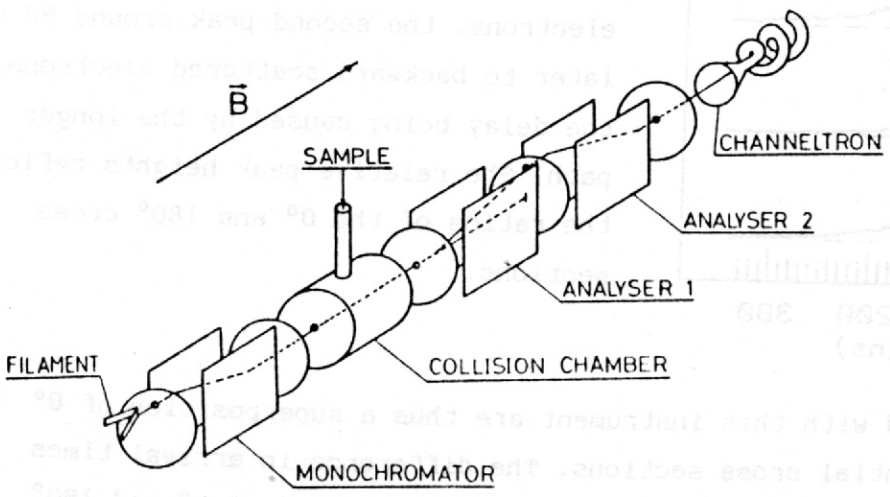

Fig. 1. Schematic diagram of the apparatus.

The use of trochoidal motion of electrons in an axial magnetic and perpendicular electrostatic fields for energy dispersion has been first reported by Stamatovic and Schulz [2] and the trochoidal analyser has subsequently often been used to prepare monoenergetic electron beams for transmission and dissociative attachment studies. The present instrument represents a successful implementation of this device to analyse the energies of the scattered electrons. The crucial feature of the present instrument is the use of two analysers in series. This arrangement permits the attenuation of the intense unscattered electron beam which also enters the analyser in the magnetically collimated instruments with their 180° geometry, and causes a large background of stray electrons in instruments using only a simple analyser stage.

On the first thought it would appear that the instrument measures the 0° scattered electrons. Experiments measuring the arrival times of the scattered electrons obtained with a pulsed incident beam have shown, however, that the backward scattered electrons are efficiently reflected on the potential barrier near the monochromator exit, traverse the target chamber a second time, also enter the analyser and are detected. The outcome of this experiment is shown in Figure 2.

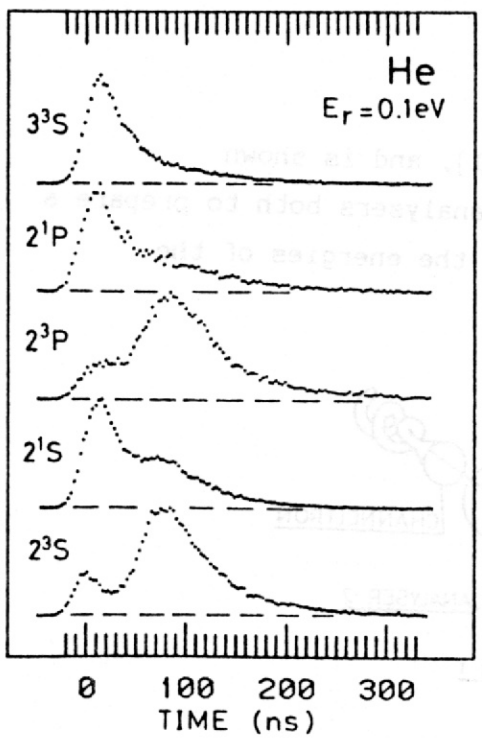

Fig. 2. Spectra of arrival times of scattered electrons after excitation by a pulsed incident beam. The energy losses were set to excitation of the specified electronic states of helium. The first peak in the arrival times is caused by the forward scattered electrons, the second peak around 80 ns later to backward scattered electrons, the delay being caused by the longer path. The relative peak heights reflect the ratios of the 0° and 180° cross sections.

The data obtained with this instrument are thus a superposition of 0° and 180° differential cross sections. The difference in arrival times could in principle be used to measure the exact ratios of 0° and 180°

cross sections and thus extend the range of angular dependence measurements to 180°.

The trochoidal electron spectrometer may also be used to record electron transmission spectra (ETS). In this mode the analyser is not used; all its elements are connected together and used as a collector of the total electron current emerging from the target chamber. In the energy-loss mode, even without the capacity to vary the scattering angle, the triplet states may be observed with low residual energies, and dipole forbidden, spin allowed transitions appear with intermediate residual energies.

The probability to excite any of these states as a function of incident electron energy is measured by the energy-dependence spectra. An example, the probability to excite the v=14 level of the electronic ground state of N_2, is shown in Figure 3.

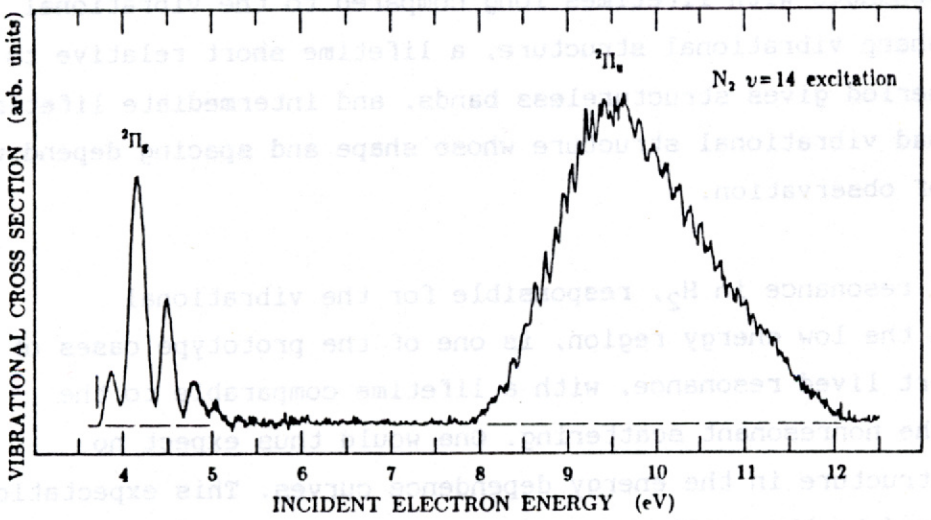

Fig. 3. Energy dependence of exciting the v=14 level of the electronic ground state of N_2.

The peaks below 5 eV are caused by the tail of the $^2\Pi_g$ resonance which was also visible in the transmission spectrum. The broad structured band in the 8-12 eV range is caused by the $^2\Pi_u$ core excited resonance [3], with double occupancy of the π^* orbital.

In the conclusion of this section several advantages and drawbacks of the present instrument in comparison with an electrostatic apparatus may be recognized. Among the drawbacks is the inability to vary the scattering

angle. The resolution of the instrument, about 35 meV, suffices to resolve the vibrational structure in most cases, but is less than the best obtained with electrostatic instruments. These drawbacks are more than outweighted by several advantages for a number of applications. Most important is the high sensitivity, which appears to surpass that of the electrostatic instruments by several orders of magnitude. Second is the low energy capability; both the incident and the scattered electron energies may be varied down to 30 meV. The energy dependence spectra are relatively easy to correct for the instrumental transmission function. In addition there are some practical advantages like low sample consumption and the capability of the instrument to record both the transmission and the energy-loss spectra.

3. RESONANT VIBRATIONAL EXCITATION IN H_2 and N_2.

The shape of bands in the energy dependence of resonant vibrational excitation by electron impact is known to be a function of the resonant lifetime. Resonances with lifetimes long compared to the vibrational period have sharp vibrational structure, a lifetime short relative to the vibrational period gives structureless bands, and intermediate lifetimes result in broad vibrational structure whose shape and spacing depend upon the channel of observation.

The $^2\Sigma_u^+$ resonance in H_2, responsible for the vibrational excitation in the low energy region, is one of the prototype cases of an extremely short lived resonance, with a lifetime comparable to the duration of the nonresonant scattering. One would thus expect no vibrational structure in the energy dependence curves. This expectation seemed confirmed by the available experimental data (Ehrhardt et al. [4], Trajmar et al. [5]).

Mündel, Berman, and Domcke [6] recently reported a theoretical study of vibrational excitation and dissociative attachment in H_2 employing a sophisticated treatment of the nuclear dynamics. A striking result of this study, contradicting the intuitive expectation outlined above, is a prediction of a pronounced vibrational structure in the energy dependence of the excitation of the higher vibrational levels ($v > 3$). The present experiment is testing the unexpected theoretical prediction experimentally [7].

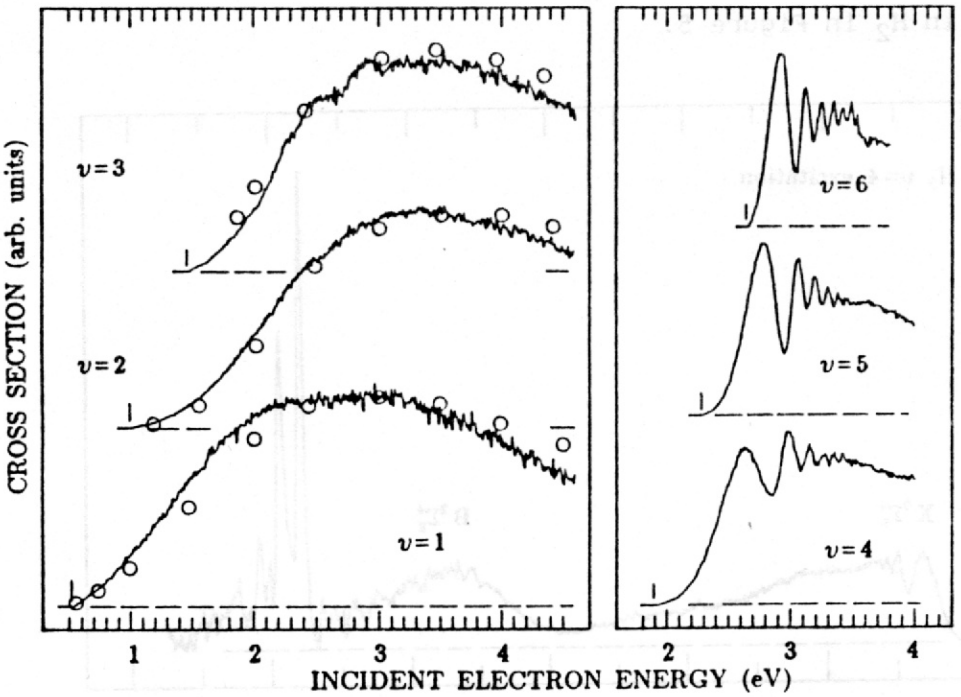

Fig. 4. Vibrational excitation cross sections in H_2. The curves are not on the same vertical scale; the relative intensities at curve maxima were given in Ref. [7]. The short vertical bars indicate threshold energies. The circles show the integral cross sections of Ehrhardt et al. [4], normalised to the present curves at the maximum of the v=1 cross section.

The experimental energy dependence curves are shown in Figure 4. The shapes of the first three curves are in a good agreement with the data of Ehrhardt et al. [4]. The striking feature are the structures observed in the curves with v = 3 and higher, putting the theoretical predictions of Mündel et al. [6] into an excellent semiquantitative agreement with the experiment. In agreement with the prediction the structure is barely visible in the v = 3 curve and becomes progresively deeper with increasing v. Revealing is the comparison of the experimental curves with the results of the three approximations, given by Mündel et al. The adiabatic nuclei approximation does not reproduce the vibrational structure, the local-complex-potential model gives structure in the cross section, its shape is, however, qualitatively incorrect and the cross section does not have the correct magnitude. The results thus emphasize the necessity of moving beyond the local approximation for proper treatment of nuclear dynamics in H_2.

This section is concluded with the global view of the vibrational

excitation in H_2 in Figure 5.

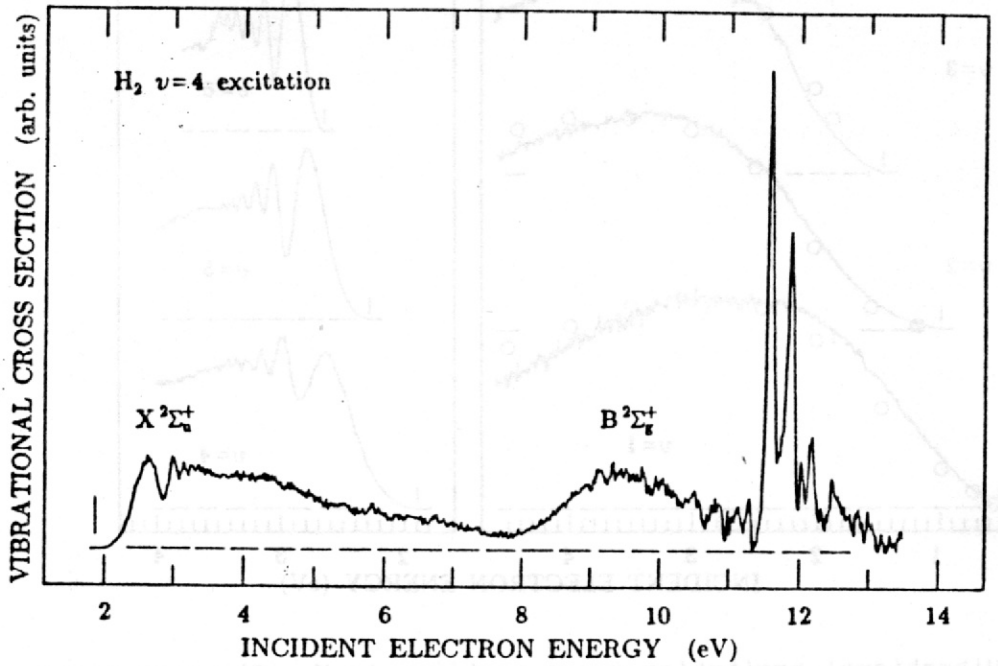

Fig. 5. A global view of the energy dependence of exciting v=4 in H_2.

In the 8-11 eV region vibrational excitation is caused by the $^2\Sigma_g^+$ core excited shape resonance, the sharp peaks above 11 eV are caused by Feshbach resonances.

The efficient vibrational excitation of N_2 by electron impact in the 2.3 eV region was among the earliest observed manifestations of resonances in electron molecule scattering. After the advent of high resolution electron impact spectrometers Schulz [8] found an unusual vibrational structure in the excitation cross sections, with the shape, position, and spacing of the peaks being dependent upon the channel of observation. The explanation of this phenomenon in terms of the "boomerang model" by Birtwistle and Herzenberg [9] was one of the most impressive successes of the theory of resonant electron - molecule scattering. The vibrational excitation in the $^2\Pi_g$ resonance region was then further studied by Ehrhardt and Willmann [10] and the measurements were extended up to v = 10 by Boness and Schulz [11]. Schulz [12] and Trajmar et al. [5] extensively reviewed the existing experimental work.

The electron-N_2 scattering in the 2.3 eV $^2\Pi_g$ resonance region has become a touchstone for the theories of the coupling of the electronic and nuclear motions, and there are numerous publications on this subject, reviewed for example by Schulz [12], Lane [13], and Herzenberg [14]. The

subject remains to be of current interest, as is shown by the recent studies, for example by Le Dourneuf and Launay [15], Berman et al. [16], Domcke et al. [17], Nestman and Peyerimhoff [18], and Morgan [19].

The vibrational cross sections obtained with the present instrument are shown in Figure 6 [20].

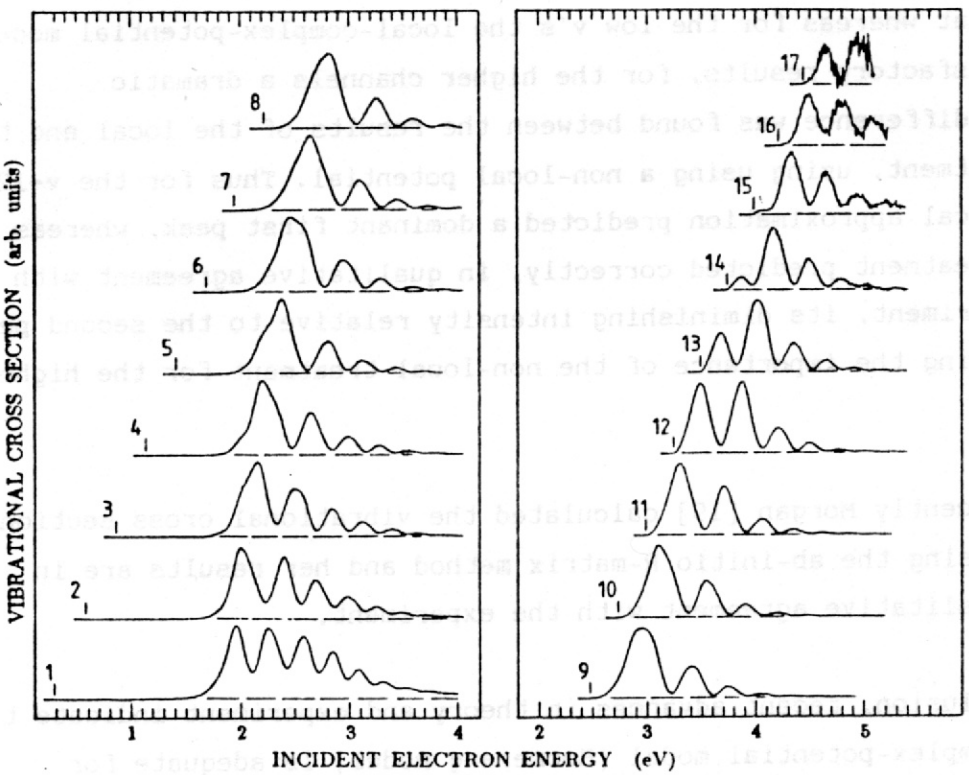

Fig. 6. Vibrational excitation cross sections for the 0→v transitions in N_2. Thresholds are indicated by vertical lines. The curves are not on the same vertical scale; the relative intensities at the curve maxima were given in Ref. [20].

The curves for v = 0 → 1 to v = 0 → 10 excitations agree well with the data of Schulz [8], Ehrhardt and Willmann [10], and Boness and Schulz [11]. In the v = 1 - 10 range the qualitative trends observed with increasing channel are (i) an increasing spacing between the peaks and (ii) an increasing dominance of the first peak in width and intensity. For v = 2 to v = 10 the first peak exhibits a "substructure" in form of shoulders. These essential features were correctly reproduced by several theoretical treatments, e.g. of Domcke and Cederbaum [21], Dubé and Herzenberg [22], and Schneider et al. [23]. For v = 11 - 17 the above mentioned trends are not continued. With the first peak approaching the threshold the peak spacing diminishes, the first peak becomes narrower, is

no longer dominant in intensity and does not exhibit the "substructure". The discussion by Cederbaum and Domcke [24] of resonant scattering in the context of both the non-local and the local potentials was until very recently the only theoretical study applicable to N_2 in this final channel range. These authors calculated the vibrational cross sections up to v = 12 for an exactly solvable model whose parameters were chosen to simulate the $^2\Pi_g$ resonance in N_2. An important conclusion of this study was that whereas for the low v's the local-complex-potential model yielded satisfactory results, for the higher channels a dramatic qualitative difference was found between the results of the local and the "exact" treatment, using using a non-local potential. Thus for the v=12 curve the local approximation predicted a dominant first peak, whereas the non-local treatment predicted correctly, in qualitative agreement with the present experiment, its diminishing intensity relative to the second peak, thus confirming the importance of the non-local treatment for the higher channels.

Very recently Morgan [19] calculated the vibrational cross sections up to v=19 using the ab-initio R-matrix method and her results are in excellent qualitative agreement with the experiment.

In conclusion, recent advances in theory and experiment indicate that the local-complex-potential model (Boomerang model) is adequate for resonance with moderate lifetimes and cross sections not including thresholds, for example the excitation of low vibrational levels in N_2. It has further the advantage of giving a transparent physical picture of the excitation process. It does, however, become inadequate for very short-lived resonances and near excitation threshold. In this situations the non-local potential treatment proves to be successful. The near threshold cross sections in N_2 could also be qualitatively well reproduced by the R-matrix method.

4. RESONANT AUTODETACHMENT OF FESHBACH RESONANCES IN POLYATOMIC MOLECULES.

The decay of the shape resonances in H_2 and N_2 described above resulted predominantly in the excitation of low vibrational levels, with the cross section decreasing rapidly with increasing exit channel. With reference to Figure 7 we may qualitatively view the excitation as consisting of a vertical electron attachment, followed by a relatively small relaxation of the nuclei on the potential surface of the negative

ion, followed by a vertical decay near the initial Franck-Condon region.

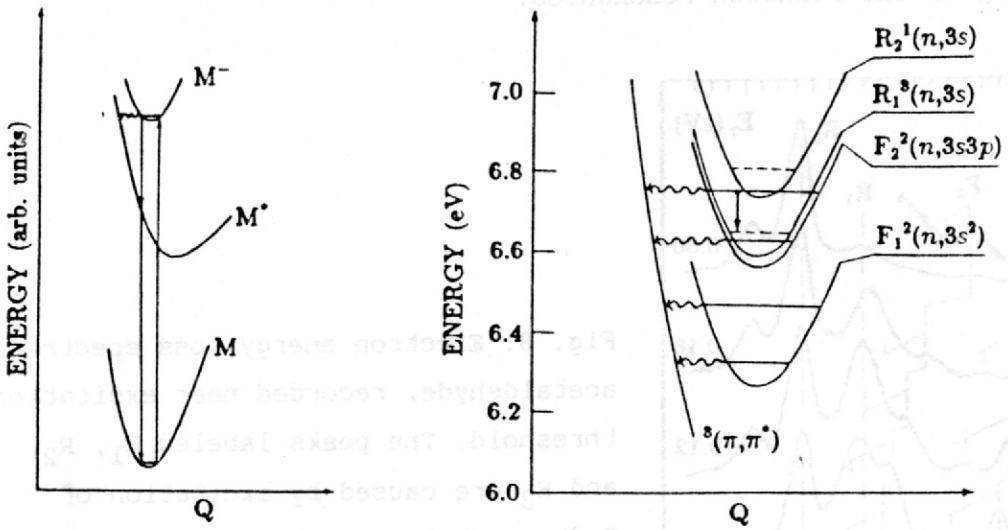

Fig. 7. Left: Schematic representation of the near-Franck-Condon detachment (vertical downward pointing arrows) and the resonant autodetachment (horizontal wavy arrow). Right: Schematic potential curves for the low-lying Rydberg states and Feshbach resonances in acetaldehyde. The horizontal wavy lines indicate the resonant autodetachment decay channel. The experiment gives no indication of the nature of the final state, the label $^3(\pi,\pi^*)$ is meant only as a possible example. The vertical arrow indicates the vibrational autodetachment channel.

This section reports the observation, that the low-lying Feshbach resonances in polyatomic molecules do not decay according to this qualitative scheme, but instead decay (quasi-)resonantly, as indicated by the horizontal wavy lines in Figure 7, resulting in emission of a very slow electron. The transition is 'horizontal', populating final states of the same energy as the resonance, which often lie in the 'Franck-Condon gaps' of the neutral molecule.

The resonant autodetachment of Feshbach resonances has been observed in many polyatomic molecules (e.g. [1,25,26]), and will be demonstrated here on the example of acetaldehyde. Acetaldehyde has two Feshbach resonances, $F_1\ ^2(n,3s^2)$ and $F_2\ ^2(n,3s3p)$, both within 0.5 eV below their $R_1\ ^3(n,3s)$ parent state. Two competing decay channels were observed for these resonances, the resonant autodetachment and the dissociative attachment [27,28]. The resonant autodetachment of these resonances is manifested in the near-threshold energy-loss spectra in

Figure 8, where peaks are observed at incident electron energies equal to the energies of the Feshbach resonances.

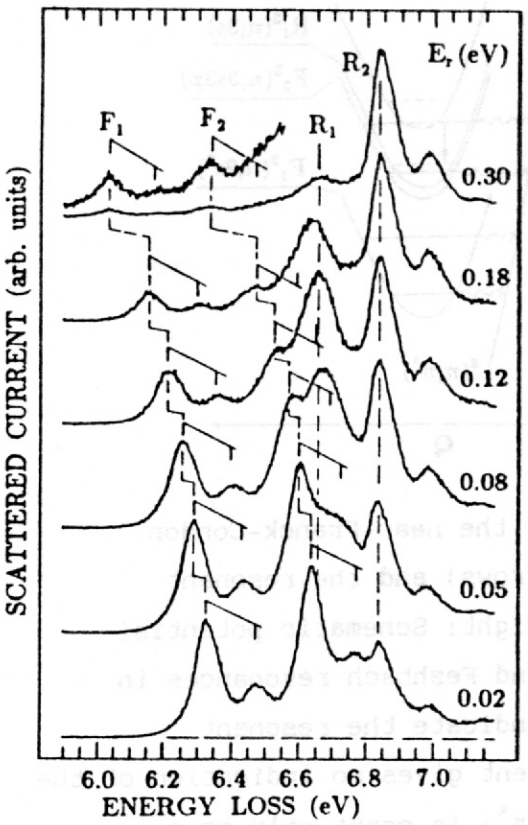

Fig. 8. Electron energy-loss spectra of acetaldehyde, recorded near excitation threshold. The peaks labeled R_1, R_2, and R_3 are caused by excitation of Rydberg states, peaks F_1 and F_2 by decay of Feshbach resonances. The Feshbach resonances are formed at fixed incident energies and the peaks caused by their decay therefore move to the left on the energy-loss scale as the residual energy is increased.

Schematic potential curves of the low-lying Rydberg states and Feshbach resonances, based upon the observations of Figure 8, are given in Figure 7. For each resonance one excited vibrational level is observed, the vibrations excited are υ_7 (CH_3 def. and C-C stretch) in F_1 and υ_6 (CCH bend) in F_2 [28]. Interestingly, the v=1 level of the F_2 resonance, at 6.76 eV, lies above the v=0 level of the $^3(n,3s^2)$ parent state at 6.65 eV, opening the possibility of vibrational autodetachment into the (electronic) parent state, as indicated by the vertical arrow in Figure 7. This decay channel actually occurs in competition with the resonant autodetachment (and dissociative attachment) and causes the high intensity of the $^3(n,3s)$ Rydberg state in the E_r=0.05-0.18 eV spectra in Figure 8.

An important question is how 'resonant' is the autodetachment, that is how close to zero are the energies of the detached electrons. Figure 9 shows the energy-distributions of the electrons emitted in the decay of the Feshbach resonances. They peak at zero and are less than 0.1 eV wide.

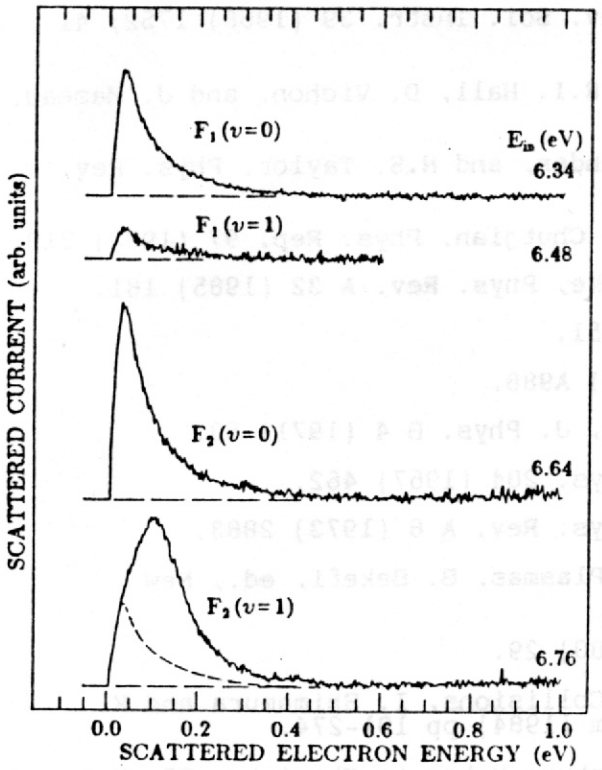

Fig. 9. Energy spectra of the electrons formed in the decay of the Feshbach resonances. All curves are on the same vertical scale. The bottom curve has been visually divided into contributions of the resonant and vibrational autodetachment channels.

In concluding this section it may be pointed out that the 'horizontal' decay of the Feshbach resonances reported here reveals very efficient coupling of the electronic and nuclear motions and is in this respect phenomenologically related to the resonant autoionization recently revealed by threshold photoelectron spectroscopy [29,30], and to fast radiationless transitions of higher excited states of polyatomic molecules. The phenomenological relation may be indicative of a related mechanism, and puts the resonant autodetachment into a broader perspective of general phenomena encountered in polyatomic molecules.

This work is part of project No. 2.219 - 0.84 of the Fonds national suisse de la recherche scientifique.

References

1. M. Allan, Helv. Chim. Acta 65 (1982) 2008.
2. A. Stamatovic and G.J. Schulz, Rev. Sci. Instr. 39 (1968) 1752; 41 (1970) 423.
3. A. Huetz, I. Cadez, F. Gresteau, R.I. Hall, D. Vichon, and J. Mazeau, Phys. Rev. A 21 (1980) 622.
4. H. Ehrhardt, D.L. Langhans, F. Linder, and H.S. Taylor, Phys. Rev. 173 (1968) 222.
5. S. Trajmar, D.F. Register, and A. Chutjian, Phys. Rep. 97 (1983) 219.
6. C. Mündel, M. Berman, and W. Domcke, Phys. Rev. A 32 (1985) 181.
7. M. Allan, J. Phys. B 18 (1985) L451.
8. G.J. Schulz, Phys. Rev. 135 (1964) A988.
9. D.T. Birtwistle and A. Herzenberg, J. Phys. B 4 (1971) 53.
10. H. Ehrhardt and K. Willman, Z. Phys. 204 (1967) 462.
11. M.J.W. Boness and G.J. Schulz, Phys. Rev. A 8 (1973) 2883.
12. G.J. Schulz, Principles of Laser Plasmas, B. Bekefi, ed., New York: Wiley (1976).
13. N.F. Lane, Rev. Mod. Phys. 52 (1980) 29.
14. A. Herzenberg, Electron-Molecule Collisions, I. Shimamura and K. Takayanagi, eds., New York: Plenum (1984) pp 191-274.
15. M. LeDourneuf and J.M. Launay, Lecture Notes in Chemistry 35, F.A. Gianturco and G. Stefani, Berlin: Springer (1984) pp 69-78.
16. M. Berman, H. Estrada, L.S. Cederbaum, and W. Domcke, Phys. Rev. A 28 (1983) 1363.
17. W. Domcke, N. Berman, H. Estrada, C. Mündel, and L.S. Cederbaum, J. Phys. Chem. 88 (1984) 4862.
18. B.M. Nestman and S.D. Peyrimhoff, J. Phys. B 18 (1985) 4309.
19. L.A. Morgan, J. Phys. B 19 (1986) L439.
20. M. Allan, J. Phys. B 18 (1985) 4511.
21. W. Domcke and L.S. Cederbaum, Phys. Rev. A 16 (1977) 1465.
22. L. Dubé and A. Herzenberg, Phys. Rev. A 20 (1979) 194.
23. B.I. Schneider, M. LeDourneuf, and Vo Ky Lan, Phys. Rev. Lett. 43 (1979) 1926.
24. L.S. Cederbaum and W. Domcke, J. Phys. B 14 (1981) 4665.
25. M. Allan, J. Chem. Phys. 80 (1984) 6020.
26. M.H. Palmer, A.J. Beveridge, I.C. Walker, and T. Abuain, Chem. Phys. 102 (1986) 63.
27. R. Dressler and M. Allan, Chem. Phys. Lett. 118 (1985) 93.
28. R. Dressler and M. Allan, J. Electron Spectrosc. Relat. Phenom., in press.
29. P.T. Murray and T. Baer, Int. J. Mass Spectrom. Ion Phys. 30 (1979) 165.
30. P.-M. Guyon and L.F.A. Ferreira, Paper presented at the Workshop on Atomic and Molecular Autoionization, Argonne National Laboratory, 1985.